R. & M. No. 2048
(6537 & 7471)
A.R.C. Technical Report

MINISTRY OF SUPPLY

AERONAUTICAL RESEARCH COUNCIL
REPORTS AND MEMORANDA

Flutter at High Incidence

By

MARY VICTORY, B.A.

LONDON : HIS MAJESTY'S STATIONERY OFFICE
Price 5s. 0d. net

Flutter at High Incidence

By

MARY VICTORY, B.A.

Communicated by the Director of Scientific Research, Ministry of Aircraft Production.

Reports and Memoranda No. 2048

January, 1943*

Summary.—This report describes work which has been done to investigate the possibility that the flexure-torsion flutter speed of a wing may be less at high incidences than at low incidences, and that this decrease may be due primarily to reduction of aerodynamic torsional damping with incidence.

The main discussion is contained in Part I, but the evidence dealt with here is obtained from tests made at relatively very low Reynolds numbers. Part II (p. 11), however, discusses the application of the results to full scale, and is based on more recent tests at larger Reynolds numbers. It is concluded that for modern aircraft the variation of critical speed with incidence is likely to be small.

PART I

1. *Introduction.*—It has long been suspected that the flutter speed of an aircraft wing at stalling incidence may be lower than at small incidences, and that any decrease is probably caused by a reduction of aerodynamic torsional damping with incidence. Evidence to support this theory has been supplied by experimental investigations using small models. In view of the fact that large accelerations are used in violent manoeuvres (particularly in pulling out of dives) high incidences may be reached at high speeds, and it has therefore been thought necessary to examine the implications of these experimental results, and to investigate the possible full-scale effects.

A detailed series of experiments was carried out by Stüder[1], who found that the flutter speeds of his models dropped considerably near the stall. This result was supported by figures quoted from National Physical Laboratory experiments by Frazer[2], and was later confirmed by Kaufmann[3]. Stüder thought that the flutter which occurred at the stall was of a different type from low-incidence flutter, and he showed that it could occur for an aerofoil with only one degree of freedom, as a pure torsional vibration. At the N.P.L. also, spontaneous pitching oscillations have been obtained about high mean incidences, when the torsional damping was negative[4], and other tests at the N.P.L.[5,6] have shown that the torsional damping may vary considerably with incidence, becoming negative near the stall.

The theoretical investigation of these results was facilitated by the fact that one of Stüder's aerofoils was very similar in shape to the aerofoil used in the N.P.L. tests to measure the variation of the aerodynamic torsional damping derivative, $(-M_{\dot{\theta}})$, with incidence, and the test conditions in the two series of experiments were almost identical. Theoretical flutter calculations have been made for Stüder's model, with flexural axis at the half chord (the N.P.L. model had oscillation axis at the half chord), using the aerodynamical derivative coefficients of R. & M. 1782[7] (corrected to infinite aspect ratio) for all the non-dimensional aerodynamic coefficients except $j_3 \left(= \frac{-M_{\dot{\theta}}}{\rho V c^3 S}\right)$; values for j_3 have been deduced from the N.P.L. tests,

* R.A.E. Report S.M.E. 3240 and addendum received 16th July, 1943.

and flutter speeds have been found giving the correct correspondence between the flutter frequency parameter $\lambda \left(= \frac{2\pi fc}{V}\right)$ and j_3. The flutter speeds thus calculated agreed very well with Stüder's experimental results at high incidences, and almost as well at low incidences, the slight disparity at small incidences being probably due to the large frequency effects occurring for low values of λ. These results suggest that at high incidences the variation of j_3 with frequency parameter and incidence is the main cause of the observed drop in flutter speeds, the effects of incidence on the other aerodynamical coefficients being negligible by comparison.

The theoretical variation of j_3 with frequency parameter has been calculated by the two-dimensional vortex theory of R. & M. 1500[8], and it is found that this variation decreases, not only as λ increases, in agreement with experiments, but also as the flexural axis is moved forwards, until at the quarter-chord position j_3 is constant for all λ values. The results of some further experiments made at the N.P.L., using a model with flexural axis at $0{\cdot}33c$, have supported this theory. It also seems probable that j_3 varies considerably with Reynolds number, and further tests are to be carried out at the N.P.L., using higher Reynolds numbers and different flexural axis positions to examine these variations in more detail.

It is concluded from the model work, experimental and theoretical, that the flutter speeds for wings near the stalling incidences can be calculated sufficiently well by classical theory, if the usually accepted value of j_3 is replaced by an experimental value depending on incidence, frequency parameter, Reynolds number, and flexural axis position.

These results have been applied to full scale, and it is shown that, owing to the range of frequency parameter values occurring in present practice, it appears unlikely that j_3 will vary much with incidence and frequency parameter. The decrease in wing flutter speeds of modern monoplanes near stalling incidences will, therefore, probably not be large, particularly as the flexural axis is usually well forward.

Experiments with propellers, mentioned by Stüder[1], showed that blade vibrations occurred particularly easily after the stall, and considerable increase of amplitude of the vibrations was observed near the negative stalling incidence ; it seems possible that the blade motion might produce a variation in the aerodynamic forces capable of increasing vibrations, and showed that pure bending oscillations could occur. It is also possible that successive stalling and unstalling of control surfaces during dives might produce stalling flutter vibrations.

High-incidence flutter of Raf wires was first observed by R. G. Harris[9] in 1921, and since then many profiles of small chord length, such as wireless masts (where the value of the frequency parameter is low owing to the small chord) have been seen to flutter with large amplitudes about stalling incidences. A theoretical investigation into this problem has been made by A. Schallenkamp[10], but further study may be necessary.

2. *Model Experiments to measure Variation of Flutter Speed with Incidence.*—Most of the experimental evidence of the variation of flutter speed with incidence has been provided by H. L. Stüder, who has reported the results of two series of experiments on this subject[1].

The first experiments were rather crude, but showed clearly that the flutter speed varied considerably with the incidence of the aerofoil. Stüder measured the critical dynamic pressure head q_k $(=\frac{1}{2}\rho V_k^2)$ for a large range of incidences, and found that near the stationary stalling angle, at which the airflow normally breaks away from the aerofoil, the critical pressure decreased very rapidly to about half its value at zero incidence. There was a phase difference of about 90 deg. between the bending and twisting oscillations, so long as the airflow had not broken down, but near the critical angle a different kind of vibration was set up, in which the flexural and torsional movements were in phase.

Stüder then examined the field of flow round the aerofoil when it oscillated about the critical incidence as mean position, and he found that the breakaway was delayed to the end of the amplitude, i.e. to an incidence appreciably greater than for the stationary aerofoil; on the

return movement re-establishment of smooth flow was also delayed. Thus, at the critical angle, the air forces on the wing depended on the direction of motion, the resistance law being, therefore, double valued, so that at this angle forced vibrations might be maintained. This supposed " hysteresis " effect was also demonstrated by Farren[11].

From these experiments Stüder concluded, tentatively, that there are two distinct kinds of wing flutter ; the first kind is the usual low-incidence flutter which obeys a single-valued force law ; the second type is associated with the breakaway of airflow from the wing, and may be caused by an " aerodynamic hysteresis " effect at the stationary stalling angle. This second kind of flutter will be referred to as " stalling flutter ".

A second series of experiments was then carried out to study the two kinds of flutter in much greater detail. Two-dimensional conditions were simulated and two degrees of freedom (corresponding to bending and twisting) were considered. Three aerofoils were used, one of symmetrical profile, one slightly cambered, and one with large camber. The torsional frequency, frequency ratio, positions of inertia and elastic axes, and the moment of inertia of each profile were varied, as far as possible independently, and for each structural combination the value of the critical dynamic pressure head, the frequency of oscillation, the flexural and torsional amplitudes, and the phase difference were measured for a complete range of angles of incidence, i.e. between the positive and negative angular limits of breakaway of flow and beyond. The range of Reynolds number used was approximately between $R = 0{\cdot}8 \times 10^5$ and $R = 3{\cdot}0 \times 10^5$, and the frequency parameter $\lambda \left(= \frac{2\pi fc}{V}\right)$ was varied between 0 and 1·0.

The results of these experiments confirmed and extended those of the first tests. In general, the flutter speed increased slowly with positive or negative incidence from no-lift until, near the stall, it dropped sharply to a value much lower than that at 0 deg. When the incidence was still further increased the flutter speed rose again fairly rapidly, the range of incidence over which the low flutter speed persisted increasing as the flexural axis was moved backward along the chord.

At incidences near the stall, where the airflow during a period of oscillation alternately followed the profile and broke away, there was a marked change in the type of flutter, shown by a sharply defined phase jump and increase of frequency, as well as change of amplitude. The phase difference between the bending and twisting oscillations dropped by about 45 deg., sometimes vanishing completely, and the flutter frequency, which had previously remained almost constant, increased sharply. If the flexural axis was well forward, the resultant frequency was higher than either of the two natural frequencies. In the limiting region between the two kinds of flutter, the vibrations were very violent, but above the stall the flutter amplitude, which had varied widely at low incidences, became very small, and predominantly torsional, often with beats.

Variation of the structural properties of the aerofoils had very different effects on the stalling flutter as compared with the low-incidence flutter. Change of inertia axis position influenced the normal flutter greatly, q_k increasing asymptotically to infinity as the inertia axis was moved forwards to coincide with the flexural axis, but had little effect on the stalling flutter; which could occur even when the inertia axis was ahead of the flexural axis, when it was impossible to obtain normal flutter. When the inertia axis position was kept constant, and the flexural axis was varied, the variation of the low-incidence flutter speed, as long as the flexural axis was ahead of the inertia axis, was not large (except when the two axes were very close, when it increased rapidly), but the stalling flutter speed decreased to a minimum when the two axes coincided. The natural frequency ratio, ζ (torsion/flexure), had little effect on the stalling flutter, for which the critical velocity was often higher at $\zeta = 1{\cdot}0$ than at other values, whereas at lower incidences there was always a minimum flutter speed when the flexural and torsional frequencies were equal.

The drop in the phase difference, when the type of flutter changed, supported Stüder's view that this stalling flutter was due to aerodynamic hysteresis, as zero phase difference would give the most favourable conditions for oscillations due to such a cause. It was suggested to Stüder that, if the stalling flutter depended on a hysteresis effect of the broken-away flow, it should be possible to obtain such oscillations in systems with only one degree of freedom and so, as a further check, he carried out some experiments allowing only freedom in torsion. The results agreed with the prediction ; pure torsional vibrations were observed in the region of the stall, while, as was expected, normal flutter could not be obtained. The value of the flutter speed, all other things being equal, was slightly lower than if both degrees of freedom were present.

Stüder finally concluded that the flutter which occurs near the stall has quite different characteristics from that occurring at low incidences, and may take place when there is only one degree of freedom, being due to aerodynamic hysteresis near the stall ; and he drew a sketch of the probable shape of the hysteresis curve of a wing vibrating with constant frequency and maximum torsional amplitude θ_0 in the region of breakaway of flow (Fig. 1).

The results of Stüder's experiments have been confirmed by other model tests. Kaufmann[3] observed the same sharp decrease in flutter speed near the stall, and the two distinct types of oscillation with the characteristics observed by Stüder ; unfortunately no data are available for Kaufmann's aerofoils, although from the values of q_K and frequency given it seems probable that the models were small and were tested at low Reynolds numbers and speeds, possibly in the same range as used by Stüder. Some experiments carried out at the N.P.L. have also shown that the flutter speed may decrease at high positive and negative incidences, and the results of these tests have been given by Frazer[2].

Other experiments at the N.P.L.[4] have provided further evidence to show that one-degree-of-freedom oscillations can arise about high mean incidences. Spontaneous pitching oscillations were obtained for an aerofoil with elastic axis at the half chord, over a range of high incidences (in one case starting below the stall), indicating that the torsional damping was negative. A subsequent series of N.P.L. experiments [5, 6] confirm that the torsional damping may vary considerably with incidence and become negative near the stall, so that such oscillations may arise. This last series of experiments is described in the following section.

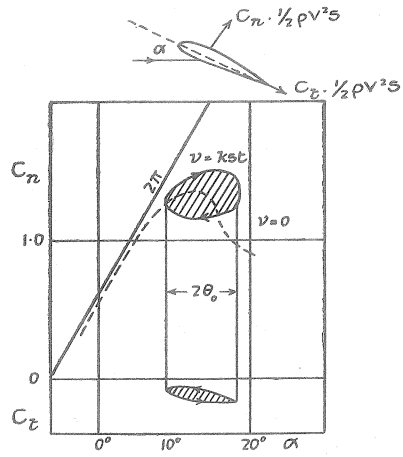

FIG. 1

3. *Model Experiments to measure Variation of Aerodynamic Torsional Damping with Incidence.* —Experiments have been carried out at the N.P.L. [5, 6] to measure the aerodynamic pitching moment derivatives at various incidences for a symmetrical aerofoil of infinite aspect ratio, oscillating about an axis at half chord. The pitching moment derivative coefficient b_1, defined as

$$b_1 = \lambda m_{\dot{\theta}} = \frac{\lambda M_{\dot{\theta}}}{\frac{1}{2}\rho V c^3 s}$$

has been measured at incidences between 0 deg. and 24 deg., a range going well above the stalling angle of the aerofoil, which is about 12 deg.

Two values of Reynolds number were used in these experiments, $R = 2{\cdot}83 \times 10^5$ and $R = 1{\cdot}42 \times 10^5$, the original tunnel speed being halved to give the second value ; for $R = 1.42 \times 10^5$ the frequency parameter $\lambda \left(= \frac{2\pi fc}{V}\right)$ was varied from 0 to 1·6, but for

$R = 2{\cdot}83 \times 10^5$, the tests could only be carried out for λ up to $0{\cdot}8$, as this gave the limiting safe frequency at the higher speed. The torsional amplitude of oscillation was varied ; three values were used at approximately 2 deg., 4 deg. and 6 deg.

From these values of b_1, the corresponding values of j_3, the torsional damping coefficient used in flutter theory, were evaluated ; j_3 is defined as

$$j_3 = -\frac{M_{\dot{\theta}}}{\rho V c^3 S} = \frac{-b_1}{2\lambda}.$$

The experimental values of j_3 at each incidence have been plotted against λ for each of the three torsional amplitudes, in Figs. 2, 3 and 4, and these curves have been cross-plotted in Figs. 5–12 to show the variation of j_3 with torsional amplitude and λ for constant incidences in the range 8 deg. to 24 deg.

These figures show that at low values of λ there is considerable variation of j_3 both with incidence and with λ, but that for higher values of λ this variation is comparatively small. When λ is less than about $0{\cdot}8$, j_3 is positive at incidences up to about $10{\cdot}0$ deg. and negative for higher incidences up to about 17 deg., i.e. 5 deg. above the stall, but as λ increases the negative values decrease rapidly towards zero, and, for λ greater that about $1{\cdot}0$, j_3 has become positive for all measured incidences up to 17 deg. As λ increases further the curves for j_3 at each of these incidences tend to flatten out, becoming almost horizontal, and the variation with incidence is comparatively small.

For incidences above 17 deg., j_3 is initially positive, but may change sign and even reach large negative values as λ increases near $\lambda = 1{\cdot}0$; this is perhaps because the aerodynamic centre of the aerofoil has moved backwards considerably. The points plotted for these incidences indicate, however, that j_3 probably becomes positive again as λ increases further, and that these curves then follow the ones for lower incidences.

It seems likely that j_3 (λ) curves at all incidences approach horizontal asymptotes as λ increases above $1{\cdot}5$; and that the variation of j_3 with incidence decreases so that j_3 probably does not fall much below its value at zero incidence. The N.P.L. hoped that the experiments might be continued at higher values of λ, by reducing the tunnel speed still further, but this proved impossible because the frictional damping in the system became large enough at lower speeds to make the results very unreliable.

The value of j_3 at any incidence is also affected by the Reynolds number, as is shown in Figs. 2, 3 and 4. It is not possible to determine the variation of j_3 with Reynolds number from the above tests, as only two values of R were used, differing only by a factor of 2 ; but it is evident that this variation may not be negligible, although it apparently diminishes as λ increases. A further series of tests is being carried out in the Compressed Air Tunnel at the N.P.L., in which much higher values of R may be reached, and the Reynolds number effect will be further studied when the results of these experiments are available.

4. *Theoretical Variation of Aerodynamic Torsional Damping Derivative Coefficient, Frequency Parameter and Flexural Axis Position and some Further Experimental Results.*—In R. & M. 1500[8] two-dimensional vortex theory is used to obtain a set of aerodynamical derivatives appropriate to small incidences in terms of the flexural axis position (expressed as h, the ratio of the distance of flexural axis behind the leading edge to the aerofoil chord) and two quantities G and H, which depend only on the frequency parameter.

Fig. 13, which is reproduced from A.D. Report No. 3163[12] shows the variation of X and Y, two functions of G and H which occur in the expression for j_3 (also given in the figure), with λ. From this figure it is evident that, except for values of h near $\frac{1}{4}$, the variation of j_3 will be large at small values of λ, below $1{\cdot}0$, but will decrease rapidly as λ increases above $1{\cdot}0$, where X and Y approach horizontal asymptotes, and j_3 becomes almost constant as λ increases.

The theoretical variation of j_3 with λ, for $h = 0{\cdot}5$, has been plotted in Fig. 2 (dotted curve) ; at small values of λ this curve follows very closely the experimental curves at low incidences, and as λ increases further it forms a mean of all the curves $j_3 = j_3\ (\lambda,\ \alpha)$. If the agreement between experiment and theory continues for higher λ, it may be said that the variation of j_3 with λ is negligible at values of λ about $1{\cdot}5$.

In Fig. 14, reproduced from R. & M. 1879[13] the variation of j_3 with flexural axis position, according to the vortex theory, has been plotted for different values of λ. This figure shows that, theoretically, the variation of j_3 with λ is influenced largely by the position of the flexural axis ; when the axis is set back at the half-chord, j_3 varies considerably with λ, at low λ values, but this variation decreases as the flexural axis is moved forwards, until, when the axis is at the quarter-chord, j_3 is constant for all λ.

If the agreement between theory and experiment is as good at other positions of the flexural axis as when this axis is at the half-chord, it is reasonable to suppose that, for more normal positions of the flexural axis, i.e. further forward, the variation of j_3 with λ would be reduced. To examine this possibility, a few further experiments have been carried out at the N.P.L., using the same aerofoil and test conditions as previously, but with the flexural axis at $0{\cdot}33c$. Theoretically, the ideal position of the flexural axis would have been at the quarter-chord, but this was ruled out because of difficulty in balancing the aerofoil.

The values of j_3 obtained in these experiments are plotted against λ in Figs. 15 and 16. Most of these tests were made using a torsional amplitude of $6{\cdot}03$ deg. (Fig. 15), and at this amplitude the curves $j_3 = j_3\ (\lambda)$ at all incidences are noticeably flatter between $\lambda = 0$ deg. and $\lambda = 1{\cdot}0$ than previously (compare with Fig. 2), showing that the variation with λ and with incidence has decreased at low values of λ, while at higher values of λ the curves again appear to approach horizontal asymptotes at positive values of j_3, and the variation with incidence becomes very small.

The vortex theory variation of j_3 with λ, for $h = \frac{1}{8}$, has been plotted in Fig. 15 (dotted curve), and again the curve has the same shape as the experimental curve at zero incidence ($-0{\cdot}27$ deg. actually), although here the values do not agree quite so well, the experimental value of j_3 at $-0{\cdot}27$ deg. being about $0{\cdot}9$ of the theoretical value at all λ values, and the vortex theory curve lies above all the experimental curves, instead of forming a mean at λ values above $1{\cdot}5$ as before.

The N.P.L. made one test at $-0{\cdot}27$ deg. incidence, using an aspect ratio equal to $4{\cdot}4$, but the curve obtained differed very little from the curve at the same incidence with infinite aspect ratio, the difference being negligible for λ greater than about $1{\cdot}0$.

A few tests were made with a torsional amplitude of $2{\cdot}02$ deg., and the curves obtained (Fig. 16) may be compared with those of Fig. 4. The variation of j_3 at low values of λ is still large, but it appears that the j_3 curves for incidences up to the stall become positive at smaller values of λ than previously (incidences up to 12 deg. become positive when $\lambda > 0{\cdot}6$, instead of $0{\cdot}7$) and there is very little variation with λ above this value.

5. *Flutter Calculations for Stüder's Aerofoil with Flexural Axis at Half-Chord, using Values of j_3 obtained from N.P.L. Experiments on a Similar Aerofoil.*—To find whether the variation of flutter speed with incidence, observed by Stüder, is related to the variation of aerodynamic torsional damping with incidence shown in the N.P.L. tests, flutter calculations have been made for Stüder's symmetrical aerofoil under certain conditions, using the fundamental aerodynamical coefficients of R. & M. 1782[7], with allowance for infinite aspect ratio, for all aerodynamical derivatives except j_3. The data used in the calculations are collected in Appendix I.

The symmetrical aerofoil was chosen because it was similar in shape to that used for the N.P.L. experiments, and was tested with several positions of the flexural axis including the half-chord position, which was that used in the N.P.L. tests. The ranges of Reynolds number

and frequency parameter used for the two aerofoils were almost the same, the N.P.L. aerofoil being tested for $R = 2{\cdot}83 \times 10^5$ and $R = 1{\cdot}42 \times 10^5$, over a range of λ values between 0 and 1·57, while for Stüder's model with flexural axis at $0{\cdot}5c$, the Reynolds number was varied between $0{\cdot}8 \times 10^5$ and $2{\cdot}4 \times 10^5$, and the range of λ values used was between 0 and 1·0.

Stüder's symmetrical aerofoil, with flexural axis at $0{\cdot}5c$, was slightly over-mass-balanced, and in this condition Stüder tested the model at several values of the torsional frequency ; for each of these values a series of tests was made using different flexural frequencies. The experimental points for one such series, where the torsional frequency used was 12·7 c.p.s., and the frequency ratio ζ, (= torsional frequency/flexural frequency) was varied between 1·06 and 2·12, are shown in Fig. 17. The critical dynamic pressure head q_K is plotted against incidence, and the sudden drop in q_K near the stall is shown clearly. The low values of q_K persist over a wide range of incidences, owing to the position of the flexural axis, and then there is a sharp rise again at about 10 deg. above the stall. This series of tests has been used for the calculations, because it is one in which Stüder obtained flutter speeds below the maximum tunnel velocity at low incidences as well as near the stall ; when the torsional frequency was increased these low-incidence flutter speeds became too high to be recorded, and the stalling flutter speeds also increased. The low-incidence flutter speeds were observed when the frequency ratio ζ (torsion/flexure) was highest, at $\zeta = 1.75$ and $\zeta = 2{\cdot}12$; this was probably owing to the flexural axis position, as when the axis was placed well forward, flutter speeds were obtained at low incidences for a range of values near $\zeta = 1{\cdot}0$. As the axis was moved backwards this ζ range shifted to higher values.

To relate the N.P.L. results to those of Stüder, flutter calculations were made for Stüder's aerofoil in the conditions described above, varying j_3 arbitrarily between 0 and 1·0 (the value of j_3 obtained by the theory of R. & M. 1782 was 0·192). From the values obtained for the calculated flutter speeds and frequencies (which are plotted in Figs. 18 and 19) a curve of flutter frequency parameter λ_c against j_3 was drawn (in Fig. 20) for each of the six frequency ratio values considered.

The theoretical flutter speed decreased with the damping, and the range of values of j_3, for which flutter could arise, decreased with the frequency fatio ζ, until $\zeta = 1{\cdot}06$, flutter was posssible only if the damping were negative. The flutter frequency changed very little with j_3, except near $j_3 = 0$, when it increased. The theoretical curves $j_3 = j_3\,(\lambda_c)$ approached horizontal asymptotes at small negative values of j_3.

The six theoretical curves of λ_c against j_3, for the six frequency ratios considered, were plotted on the same sheet as the N.P.L. experimental (j_3, λ) curves, where they cut most of the experimental curves at least once. The points of intersection were points where the correct experimental correspondence between j_3 and λ obtained for the particular incidence at which the experimental curve was plotted. Using these values of j_3, the appropriate calculated flutter speeds were obtained from Fig. 18, and have been plotted, together with λ_c values, against incidence, for each of the six test values of the frequency ratio in Figs. 21–26. Stüder's experimental flutter speeds and λ values have also been plotted in these six figures.

The agreement between the calculated and experimental flutter speeds is remarkably good. The theoretical flutter speeds drop near the stall just as did the observed flutter speeds ; the difference in incidence at which this drop occurs is undoubtedly due to the difference in stalling angle of the two aerofoils—Stüder's symmetrical aerofoil stalled at 14·5 deg. whereas the N.P.L. model had a stalling angle of 12 deg. At incidences above the stall the agreement between theory and experiment is very close, but at low incidences the agreement is not quite so good, although even here the difference is only between 30 to 33 and 26 metres/sec. (*see* Figs. 23 and 24). This small disparity is probably due to frequency effects, since, whereas at high incidences the flutter frequency parameter λ is about 1·0, a normal value, at low incidences λ has remarkably small values of about 0·2. At such small values of λ the variation of the aerodynamical coefficients with λ is large (as shown in § 4, *see* Fig. 13) so that a small difference between

experimental and calculated λ will give a larger difference between flutter speeds. Also, in the calculations, only j_3 has been varied with λ, whereas at low values of λ all the coefficients may vary considerably, and the variation of j_3 may not become predominant until higher values of λ are reached.

Calculations were made of the flutter amplitude ratios and phase differences at high and low incidences and, although inaccurate at high incidences, the results were found to agree with Stüder's results for the symmetric aerofoil (*see* Appendix II, Table 4). Flexural and torsional amplitudes were of the same order at small incidences, but near the stall the flutter became predominantly torsional, and the phase difference between the flexure and torsion decreased.

From these results it appears that the variation in j_3 with incidence and frequency parameter is sufficient by itself to account for the observed drop in flutter speed as the stall is approached ; the effects of incidence on the other aerodynamic coefficients are, therefore, probably negligibly small by comparison, although it is possible that, in their effects on critical flutter speed, they are self-cancelling.

6. *Conclusions from Model work and Applications to Full Scale.*—It is concluded, from the work described in this Report, that the flexure-torsion flutter speed of a wing decreases at high incidences, due mainly to variation in the aerodynamic torsional damping, the effects of incidence on the other aerodynamic forces having by comparison little effect on the critical flutter speed.

The aerodynamic torsional damping varies not only with incidence, however, but also with the frequency parameter λ, with flexural axis position and with Reynolds number, the first two of these factors being the most important. As λ increases, the variation of the damping coefficient j_3 with incidence and with λ decreases rapidly, until, when λ is greater than $1{\cdot}0$, the variation of j_3 with λ is negligible, and the variation with incidence is reduced such that j_3 does not fall below about 60 per cent. of its value at zero incidence for incidences up to the stall. The variation of j_3 is further reduced if the flexural axis is moved towards the quarter-chord position. The effect of Reynolds number is not yet known, and will be considered when results of further tests are available.

Thus it appears that the large decrease in flutter speed observed in the model tests at high incidences was probably mainly due to the range of values of λ which was used, (between 0 and $1{\cdot}0$), and also perhaps to the flexural axis positions, which were usually well behind the quarter-chord ($0{\cdot}5c$ in most cases), and to the small Reynolds numbers used (as, although the effect of R is not yet determined, it appears from present results that the variation of j_3 decreases as R increases).

A further result is that, as incidence is increased, j_3 tends to decrease, thus decreasing the flutter speed, usually without much effect on the flutter frequency, so that λ tends to increase, thus increasing j_3. In so far as they vary together, therefore, incidence and frequency parameter tend to have opposite offects on the flutter speed, and the resultant decrease in flutter speed, when the incidence is increased to near the stall, is not so large as might be expected, and is probably quite small if the frequency parameter is large.

Applying these results to full scale, it is concluded that the drop in flexure-torsion wing flutter speed of a modern aircraft will be small at high incidence, since for modern monoplanes the values of λ which would be obtained at low incidences are usually above $\lambda = 1{\cdot}5$, and it can be shown, by the argument of the above paragraph, that λ at high incidences will be greater than at low incidences. Further, the flexural axes of most modern aircraft are well forward, and the Reynolds numbers obtained in flight are of the order of 10^7.

To calculate a wing flexure-torsion flutter speed at high incidence, it appears from the calculations in this Report that it is sufficient to use classical theory, replacing only j_3 by an experimental value depending on incidence, frequency parameter, flexural axis position and Reynolds number.

A further series of tests are discussed in Part II of the present Report, and an estimate is made, based on these tests, of the effects on full scale.

APPENDIX I

Data used in Calculations

TABLE 1

Comparison of Structural Properties, and Test Conditions, of the N.P.L. Aerofoil and Stüder's Symmetrical Aerofoil (as used for calculations)

Data	N.P.L. Model	Stüder's Model
Shape of section	Symmetric	Symmetric
Chord c	9 in.	12 cm.
Span	40 in.	40 cm.
Thickness-chord ratio	0·15 : 1	0·156 : 1
Aspect ratio	∞ and 4·4	∞
Position of oscillation axis	0·5c	0·5c
Position of inertia axis		0·482c
Radius of gyration about oscillation axis..		0·244c
Test conditions.		
Values of Reynolds number used ..	$1{\cdot}42 \times 10^5$ and $2{\cdot}83 \times 10^5$	Varying between about $0{\cdot}8 \times 10^5$ and $2{\cdot}4 \times 10^5$
Values of frequency parameter	Between 0 and 1·57	At flutter speeds, between 0 and 1·0

TABLE 2

Test Values of Natural Frequencies and Frequency Ratio for Stüder's Aerofoil, used in calculations

Case	Torsional frequency c.p.s.	Flexural frequency c.p.s.	Frequency ratio
1	12·7	12·0	1·06
2		11·2	1·13
3		10·0	1·27
4		8·6	1·48
5		7·25	1·75
6		6·0	2·12

TABLE 3

Values of Flutter Coefficients used in Calculations for Stüder's Symmetrical Aerofoil

Flexure Coefficients	Torsion Coefficients
$A_1 = 0{\cdot}06768\rho$	$A_3 = -0{\cdot}0003655\rho$
$B_1 = 0{\cdot}01594\rho V$	$B_3 = -0{\cdot}001196\rho V$
$C_1 = l\phi$	$C_3 = 0$
$G_1 = -0{\cdot}0003655\rho$	$G_3 = 0{\cdot}0003625\rho$
$J_1 = 0{\cdot}002073\rho V$	$J_3 = J_3'\rho V$
$K_1 = 0{\cdot}042516V^2\rho$	$K_3 = m_0 - 0{\cdot}003189\rho V^2$

These coefficients were calculated from the formulae of R. & M. 1782[7], making allowance for infinite aspect ratio, and using modes suitable for a rigid aerofoil, *i.e.*—

$$f(y) = F(y) = 1.$$

The coefficients were left in terms of the air density, ρ, for convenience, as in Stüder's experiments the value of ρ differed slightly in each of the six tests (cases 1–6 of Table 2). The elastic stiffnesses were calculated from the measured natural frequencies.

APPENDIX II

Calculation of Flutter Amplitude Ratios and Phase Angles for Stüder's Symmetric Aerofoil

An attempt was made to calculate the flutter amplitude ratios and phase angles for the symmetric aerofoil, in order to compare them with Stüder's experimental values.

At high incidences, these calculations (particularly the phase angles) were inaccurate, and mean values are given in the tables below. The inaccuracies were consistent with rapid variation of phase difference and amplitude ratio, which would agree with Stüder's observations, as he was unable to measure phase angles for the symmetric aerofoil near the stall, owing to rapid changes in value, and he had to give a range of values for the flexural amplitude in this region. (Most of Stüder's results for phase angle and amplitude changes near the stall, quoted in § 2, were obtained from experiments with cambered aerofoils).

The results obtained are quoted in Table 4 below :—

TABLE 4

Case	Experiment			Theory		
	Incidence	Amplitude Ratio = Torsion/Flexure	Phase Angle	Incidence	Amplitude Ratio = Torsion/Flexure	Phase Angle
5	−1·0°	5·24	$\frac{3}{4}\pi$	0°	1·6	30°
				3·9°	1·5	30°
	13·4°	56·0	Phase angle changing rapidly	14·26°	36·0	16°
	15·1°	35·0				
6	−0·9°	5·24	$\frac{3}{4}\pi$	0°	1·4	33°
	+0·9°	4·19	$\frac{3}{4}\pi$			
	13·8°	23·3 }	Phase angle changing rapidly with flexural amplitude	14·08°	54·0	12°
	14·3	14·0 } varying rapidly				
	14·6	47·6 }				

PART II

1. *Introduction.*—In Part I it was shown that observed decreases in flexure-torsion flutter speeds of small model aerofoils at incidences near the stall could be accounted for by the variation of the aerodynamic torsional damping with incidence. It was also shown that aerodynamic damping varies, not only with incidence, but with frequency parameter λ, Reynolds number, and flexural axis position.

Unfortunately, the experimental values obtained for the torsional damping coefficient j_3, all referred to low values of λ (between 0 and 1·5) and of R (R of the order of 10^5), and so the above conclusions could not be extended to cover possible full-scale effects.

Experiments have now been made[14, 15] at the N.P.L. to measure j_3 at values of λ between 1·0 and 3·5, with Reynolds number varied between $0{\cdot}3 \times 10^6$ and $4{\cdot}0 \times 10^6$; aspect ratios of 4·8 and 6·0 have been used, with the flexural axis situated at $0{\cdot}5c$ and $0{\cdot}33c$ behind the leading edge.

The results of these latest experiments are used here to discover whether there is likely to be any large variation of wing flexure-torsion flutter speeds of modern aircraft with incidence.

2. *Experimental Results.*—The values of j_3 quoted in Part II are obtained from recent N.P.L. experiments[14, 15], and refer to a symmetrical aerofoil (N.A.C.A. 0015) oscillating with amplitude $\theta_0 = 4{\cdot}0$ deg. Two values of the aspect ratio (4·8 and 6·0) were used, and the flexural axis position was either at $0{\cdot}33c$ or $0{\cdot}5c$ behind the leading edge.

Figs. 27, 28 and 29 show the variation of j_3 with incidence and frequency parameter, at various Reynolds numbers. These graphs are plotted on the same scale as the corresponding figures for Part I (Figs. 2, 3, 4 and 15), which referred to two-dimensional conditions at much lower values of R, and $\lambda < 1{\cdot}5$. Considering the two sets of figures it appears that—

(*a*) The variation of j_3 with incidence decreases as λ increases, and is always small for values of λ greater than 2·0, except possibly for angles of incidence far beyond the static stall.

(*b*) The variation of j_3 with incidence and with λ decreases steadily as the Reynolds number increases. For a normal position of the flexural axis in a modern aircraft wing (at 0·33 chord) the variation is negligible for λ above 1·0 and R above $2{\cdot}0 \times 10^6$, i.e. is negligible in the practical range for flight.

(*c*) The variation of j_3 with incidence, for values of λ between 1·5 and 3·0 (i.e., over the practical range), is rather less for a flexural axis position at $0{\cdot}33c$ than at $0{\cdot}5c$, particularly at higher values of R.

To show the variation of j_3 with R more clearly, the points have been replotted on a larger scale in Figs. 30, 31 and 32 to show the variation of j_3 with λ and R at various incidences. From these graphs it may be seen that the variation of j_3 with R is very small, and decreases as R increases, tending to reduce the variation of j_3 with λ.

To see how much j_3 decreases before the stall is reached, it is interesting to plot the ratio $j_3/\bar{j}_3$ against incidence α, where $\bar{j}_3$ is the value at zero incidence and j_3 is the current value. Fig. 33 shows such curves for the aerofoil with flexural axis at $0{\cdot}33c$, and the full results for the values of this ratio at the stall are given in the tables of Appendix III. From these tables it is easily seen that at the highest values of R measured, and probably for values of R approaching those of flight incidence, the decrease in j_3 is small for practical values of λ at angles below the stall, and there seems no possibility of j_3 changing sign until the incidence is well beyond the stall.

For values of λ below 1·0, which will be encountered in the flutter of small chord aerofoils such as propellers, it appears that the variation of j_3 with incidence probably decreases as R increases, but will still be considerable at practical values of R.

3. *Conclusions.*—For values of λ greater than 1·0 and R greater than 10^6, there seems no possibility that j_3 will vary appreciably with incidence up to the stall. It is therefore concluded that the variation of wing flexure-torsion flutter speed with incidence for modern aircraft is likely to be unimportant.

For values of λ less than 1·0, j_3 may still vary considerably with incidence at values of R well above 10^6, and accordingly the variation of flutter speed with incidence remains a practical problem for small-chord aerofoils.

LIST OF REFERENCES

Part I

No.	*Author*	*Title*
1.	H. L. Stüder..	Experimental Investigation of Wing Flutter. A.R.C. 2777. Dec., 1936. (Unpublished.)
2.	R. A. Frazer	Notes on the Influence of Abnormal Incidences on Wing Flutter. A.R.C. 4297. Dec., 1939. (Unpublished.) —
3.	W. Kaufmann	On the Conditions of Similitude for Model Tests on Wing Flutter. A.R.C. 4126. Sept., 1939. (Unpublished.)
4.	J. B. Bratt, K. C. Wight and A. Chinneck	Free Oscillations of an Aerofoil about the Half Chord Axis at High Incidences, and Pitching Moment Derivatives for Decaying Oscillations. R. & M. 2214. September, 1940.
5.	J. B. Bratt and C. Scruton	Measurements of Pitching Moment Derivatives for an Aerofoil Oscillating about the Half Chord Axis. R. & M. No. 1921. November, 1938.
6.	J. B. Bratt, K. C. Wight and V. J. Tilly..	The Application of a "Wattmeter" Harmonic Analyser to the Measurement of Aerodynamic Damping for Pitching Oscillations. R. & M. 2063. May, 1942.
7.	W. J. Duncan and H. M. Lyon	Calculated Flexural-torsional Flutter Characteristics of some Typical Cantilever Wings. R. & M. 1782. (1937.)
8.	W. J. Duncan and A. R. Collar	Calculation of the Resistance Derivatives of Flutter Theory, Part I. R. & M. 1500. (1932.)
9.	R. G. Harris	Rafwire Vibrations. R. & M. 759. (1921.)
10.	A. Schallenkamp	Flutter Calculations for Profiles of Small Chord. R.T.P. Trans. No. 1556. A.R.C. 6219. Oct., 1942. (Unpublished.)
11.	W. S. Farren	The Reaction on a Wing, whose Angle of Incidence is Changing Rapidly. R. & M. 1648. (1935.)
12.	G. A. Naylor	Some Theoretical Comments on Recent Results of the N.P.L. Model Tests on Wing Flutter. R.A.E. Report No. A.D. 3163. A.R.C. 5047. Jan., 1941. (Unpublished.)
13.	A. G. Pugsley and G. A. Naylor	The Influence of Wing Flexural Axis Position and Aerodynamic Torsional Damping upon Wing Flutter. R. & M. 1879. March, 1939.

Part II

14.	J. B. Bratt, W. G. Raymer and C. J. W. Mills.	Interim Note on the Measurement of Torsional Derivatives in the Compressed Air Tunnel. A.R.C. Report 6339, O.305. December, 1942. (Unpublished.)
15.	J. B. Bratt, W. G. Raymer and C. J. W. Mills.	Interim Report on Further Measurements of Torsional Damping in the Compressed Air Tunnel. A.R.C. Report 6716, O.339. May, 1943. (Unpublished.)

APPENDIX III

Tables showing the values of the ratio $j_3 / \bar{j}_3$ at the stalling angle for a symmetrical aerofoil with various aspect ratios and Reynolds numbers.

($\bar{j}_3$ is the value of j_3 at zero incidence).

(1) *Aspect ratio* $= 4{\cdot}8$, $\theta_0 = 4{\cdot}0$ deg.

(a) *Elastic axis at* $0{\cdot}33c$

λ	$R=0{\cdot}3\times10^6$	$1{\cdot}0\times10^6$	$2{\cdot}0\times10^6$
1·0		0·74	0·83
1·5	0·73	0·90	0·94
2·0	0·84	0·99	1·06
2·5	0·98	1·15	1·18
3·0	1·09	1·24	1·28

(b) *Elastic axis at* $0{\cdot}50c$

λ	$R=0{\cdot}3\times10^6$	$1{\cdot}0\times10^6$	$2{\cdot}0\times10^6$
1·0		0·69	0·76
1·5	0·58	0·76	0·81
2·0	0·72	0·86	0·91
2·5	0·93	1·01	1·04
3·0	1·02	1·13	1·11

(2) *Aspect ratio* $= 6{\cdot}0$, $\theta_0 = 4{\cdot}0$ deg.

Elastic axis at $0{\cdot}50c$

λ	$R=0{\cdot}3\times10^6$	$1{\cdot}0\times10^6$	$2{\cdot}0\times10^6$
1·0	0·60	0·75	0·83
1·5	0·65	0·84	0·84
2·0	0·74	0·94	0·95
2·5	0·88	1·01	1·03
3·0	1·0	1·13	1·13

(3) *Aspect ratio* $= \infty$, $\theta_0 = 6{\cdot}0$ deg.

(a) *Elastic axis at* $0{\cdot}33c$

λ	$R=0{\cdot}142\times10^6$
0·314	−1·4
0·628	−0·45
0·942	0·30
1·257	0·58
1·573	0·72

(b) *Elastic axis at* $0{\cdot}50c$

λ	$R=0{\cdot}14\times10^6$	$0{\cdot}283\times10^6$
0·157		−2·2
0·314		−1·65
0·628	−0·4	0
0·942	+0·57	
1·257	0·82	
1·573	0·75	

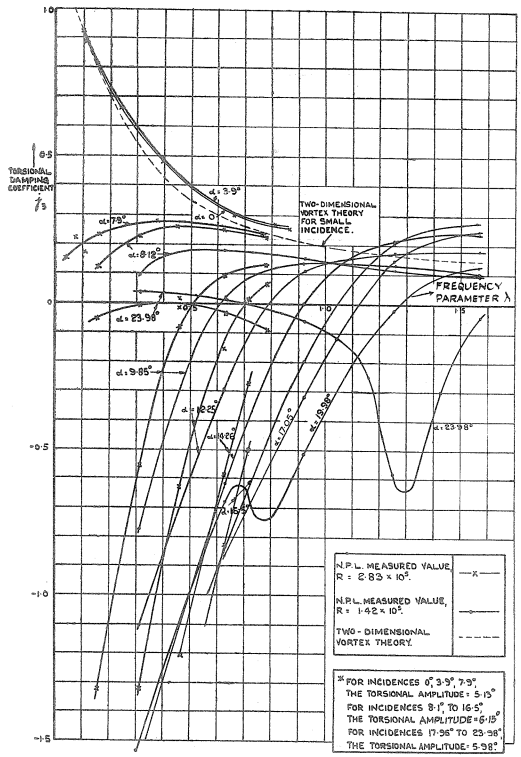

FIG. 2. Variation of Torsional Damping Coefficient f_3 with Frequency Parameter λ and with Incidence $\alpha°$ when Torsional Amplitude of Oscillation is approximately *6°, and Elastic Axis is at $0{\cdot}5c$.

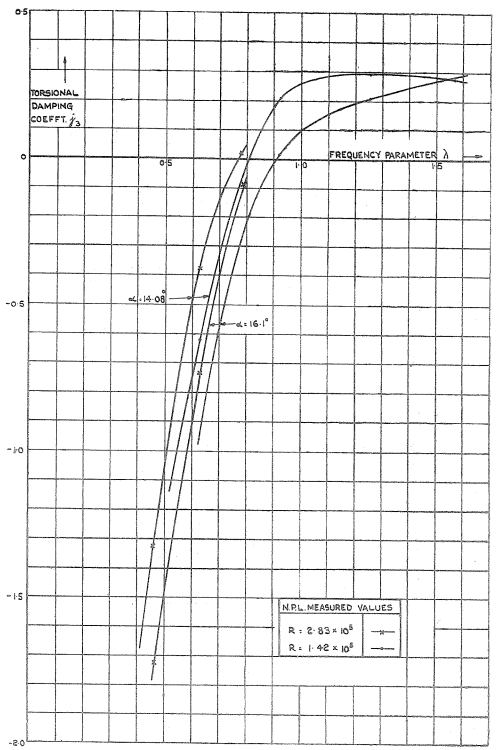

FIG. 3. Variation of Torsional Damping Coefficient f_3 with Frequency Parameter λ and with Incidence when Amplitude of Oscillation is 4·03°, and Elastic Axis is at $0{\cdot}5c$.

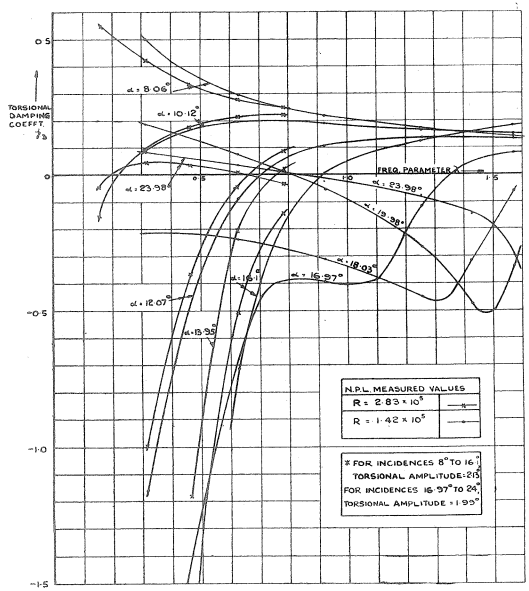

FIG. 4. Variation of Torsional Damping Coefficient j_3 with Frequency Parameter λ and with Incidence when Torsional Amplitude of Oscillation is approximately *2°, and Elastic Axis is at $0{\cdot}5c$.

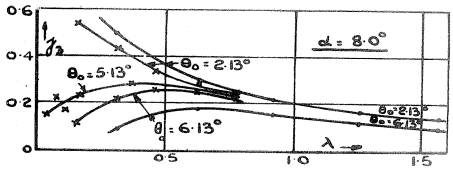

FIG. 5

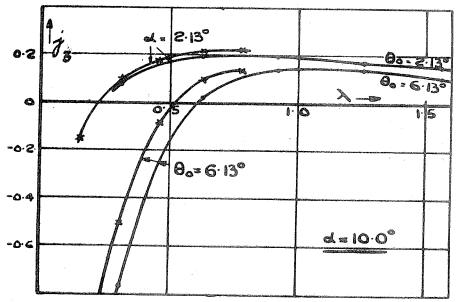

FIG. 6

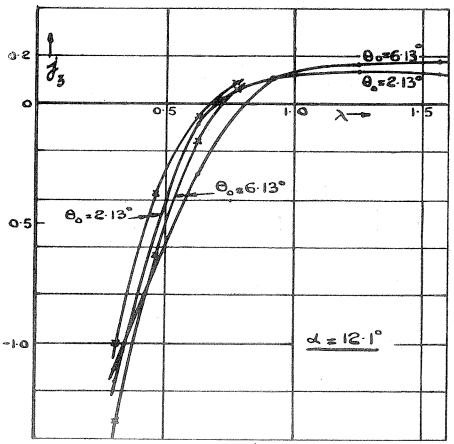

FIG. 7

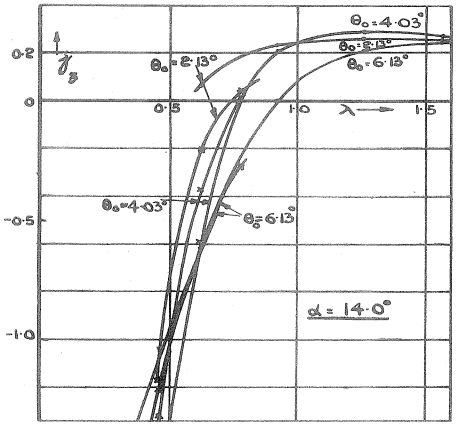

FIG. 8

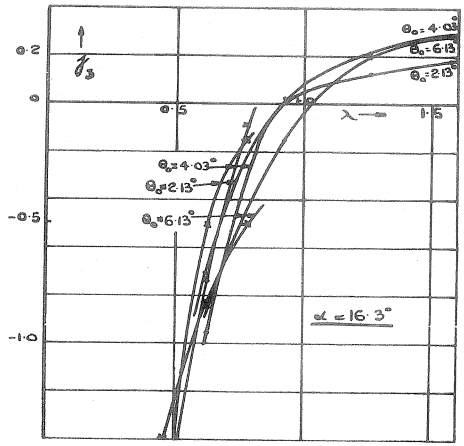

FIG. 9

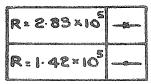

Variation of j_3 with Torsional Amplitude of Oscillation $\theta_0°$, and with λ, at Various Angles of Incidence $\alpha°$.

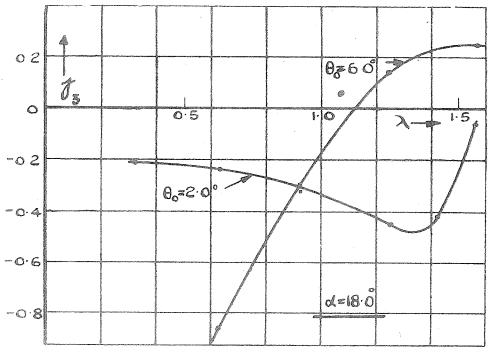

FIG. 10

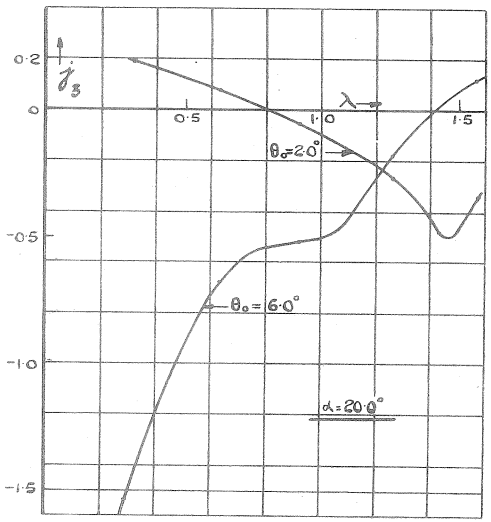

FIG. 11

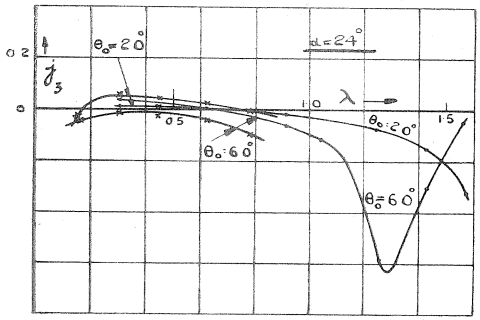

FIG. 12

R = 2·83 × 10^5	—×—
R = 1·42 × 10^5	—•—

Variation of j_3 with Torsional Amplitude of Oscillation θ_0, and with λ, at Various Incidences.

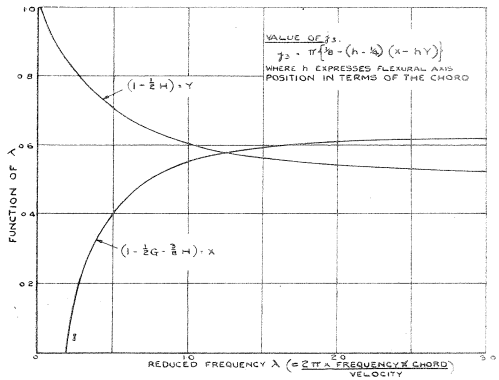

FIG. 13. Variation of X & Y with λ on Two-Dimensional Vortex Theory.

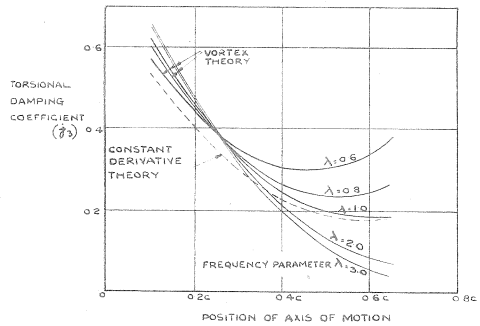

FIG. 14. Variation of j_3 with Flexural Axis Position on Two-Dimensional Vortex Theory.

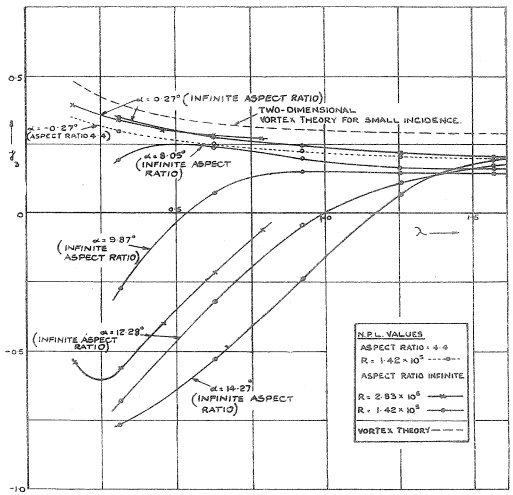

FIG. 15. Variation of Torsional Damping Coefficient j_3 with Frequency Parameter λ, when Torsional Amplitude of Oscillation = 6·03° and Flexural Axis is at 0·33c. (N.P.L. Experimental Values compared with Vortex Theory.)

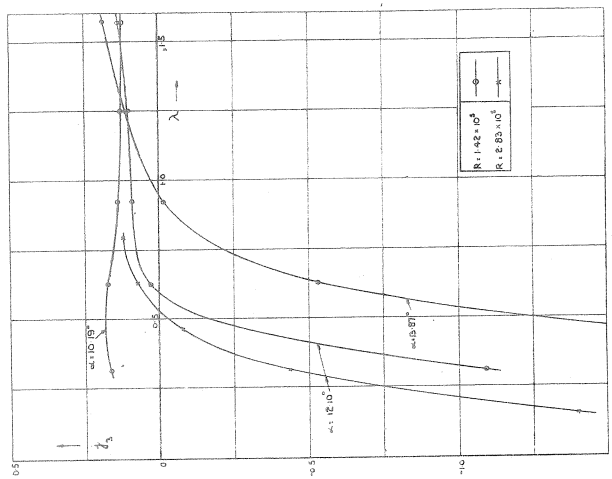

FIG. 16. Variation of Torsional Damping Coefficient j_β with Frequency Parameter λ when the Torsional Amplitude of Oscillation is 2·02° and the Flexural Axis is at 0·33c. (N.P.L. Experimental Points.)

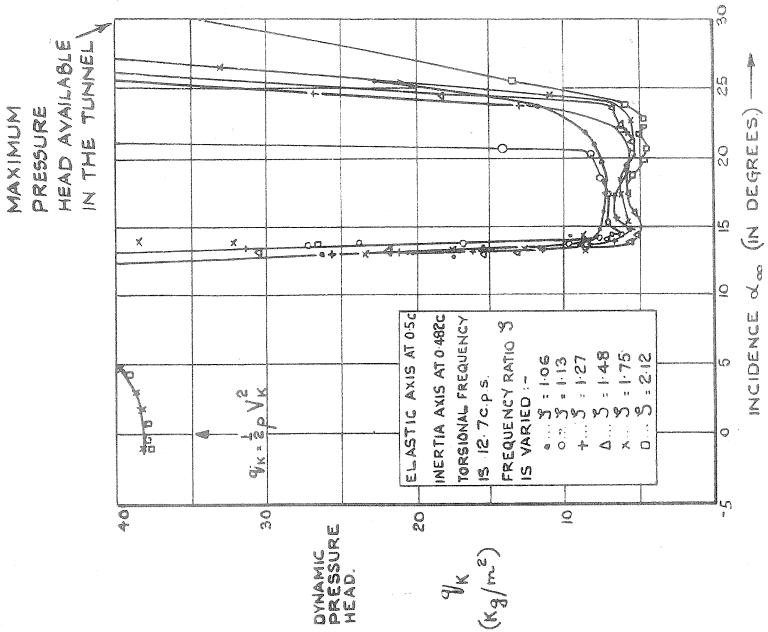

FIG. 17

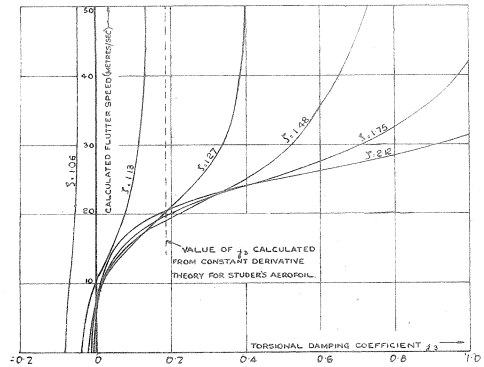

FIG. 18. Variation with j_3 of Calculated Flexure-Torsion Flutter Speed of Stüder's Symmetrical Aerofoil.

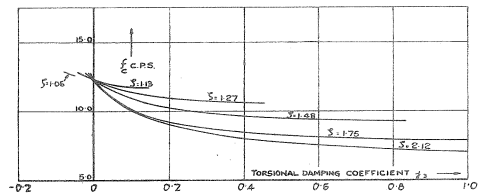

FIG. 19. Variation with j_3 of Calculated Flexure-Torsion Flutter Frequencies for Stüder's Symmetrical Aerofoil.

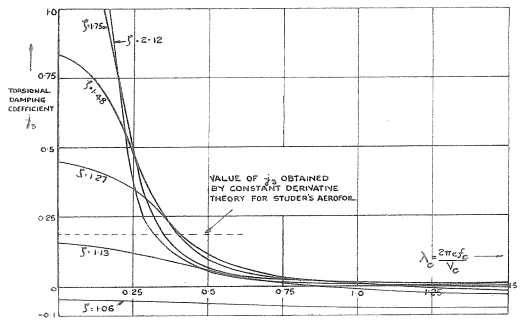

FIG. 20. Calculated Variation of λ_c with j_3 for Stüder's Symmetrical Aerofoil.

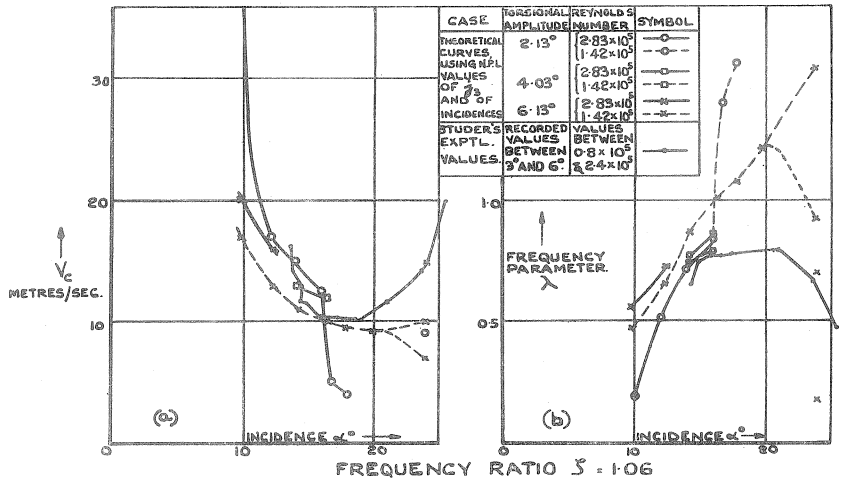

FIG. 21

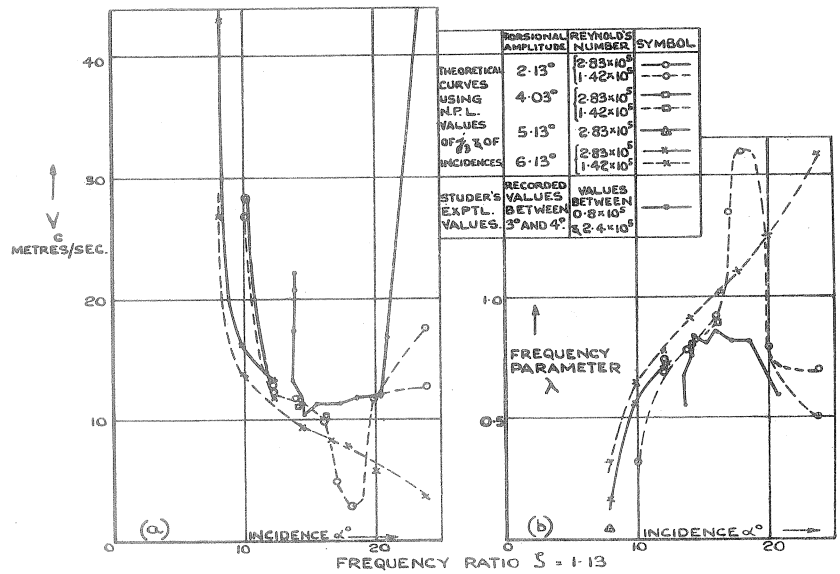

FIG. 22

FIGS. 21–22. Comparison for Six Values of the Frequency Ratio ζ of Stüder's Experimental Values of Flutter Speed V_c and Frequency Parameter λ, at Various Incidences, with Values obtained by using the Calculated Variation of V_c and λ with j_3 in Conjunction with the N.P.L. Measured Variation of j_3 with Incidence.

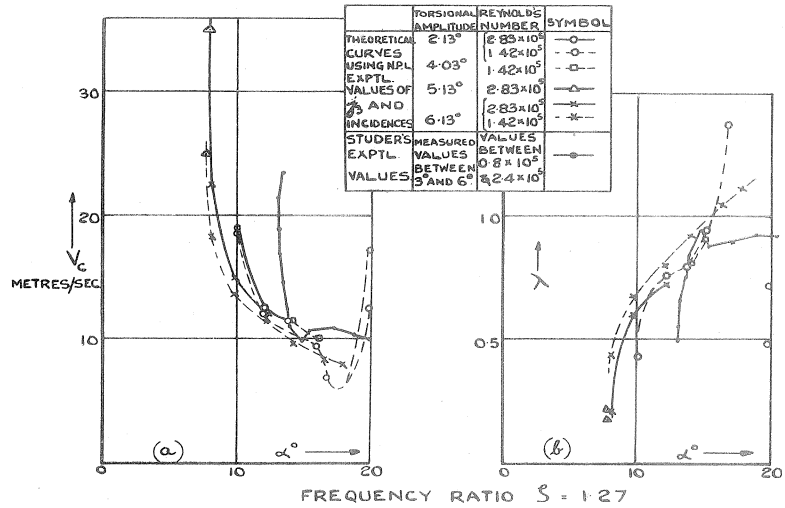

FIG. 23

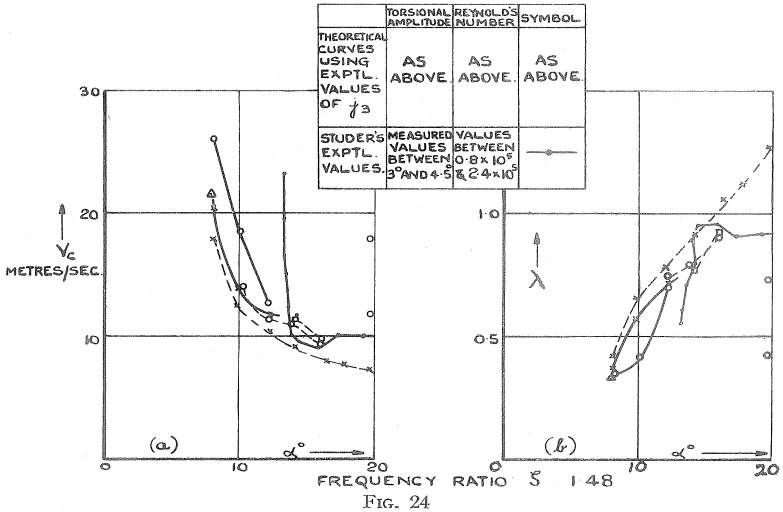

FIG. 24

FIGS. 23–24. Comparison for Six Values of the Frequency Ratio ζ of Stüder's Experimental Values of Flutter Speed V_c and Frequency Parameter λ, at Various Incidences, with Values obtained by using the Calculated Variation of V_c and λ with f_3 in Conjunction with the N.P.L. Measured Variation of f_3 with Incidence.

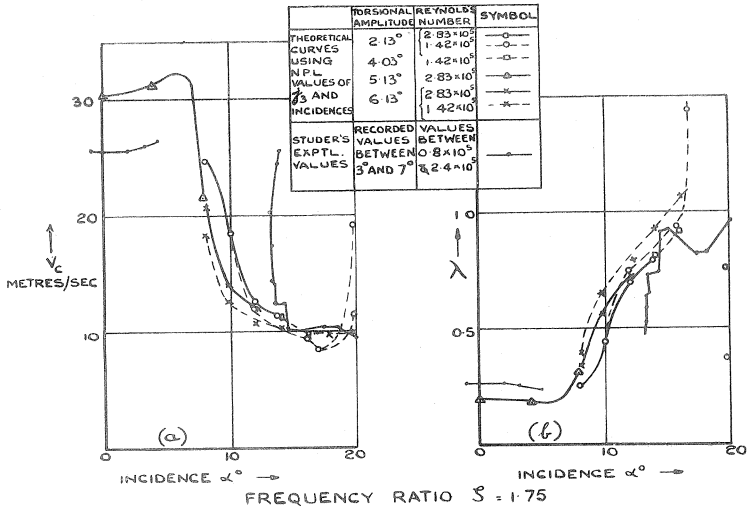

FREQUENCY RATIO ζ = 1·75

FIG. 25

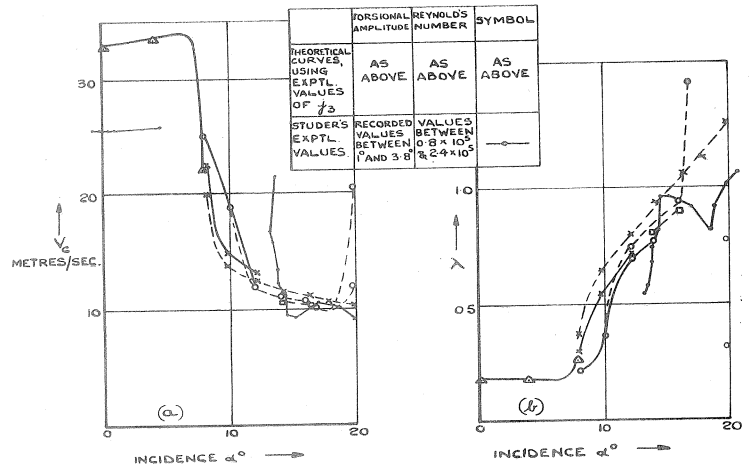

FREQUENCY RATIO ζ = 2·12

FIG. 26

FIGS. 25–26. Comparison for Six Values of the Frequency Ratio ζ of Stüder's Experimental Values of Flutter Speed V_c and Frequency Parameter λ, at Various Incidences, with Values obtained by using the Calculated Variation of V_c and λ with j_3 in Conjunction with the N.P.L. Measured Variation of j_3 with Incidence.

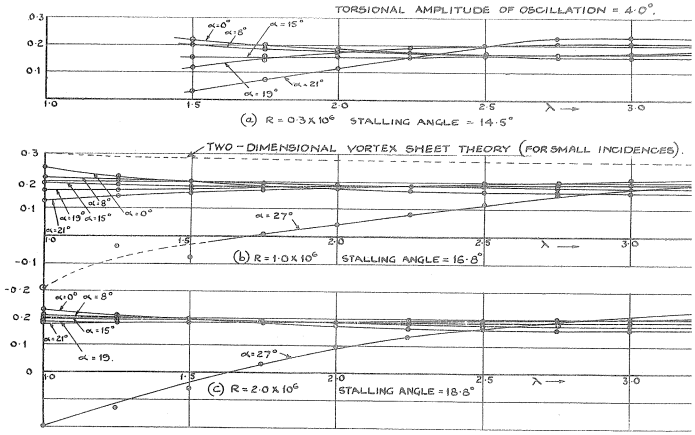

FIG. 27. Variation of j_3 with Incidence and Frequency Parameter Various Reynolds numbers for an N.A.C.A. 0015 Aerofoil with Aspe Ratio = 4·8, and Elastic Axis at 0·33*c*.

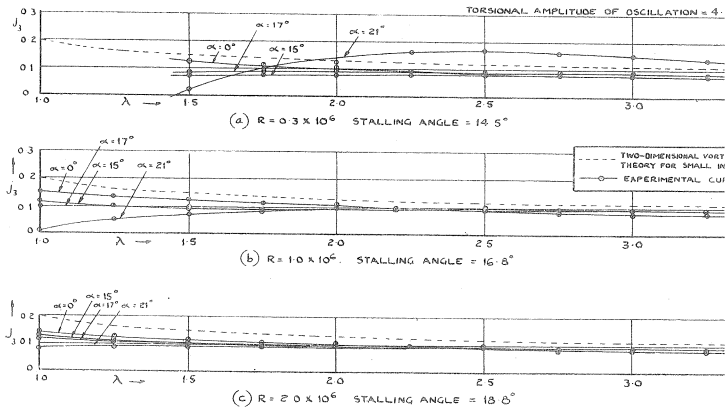

FIG. 28. Variation of j_3 with Incidence and Frequency Parameter, at V Reynolds numbers for an N.A.C.A. 0015 Aerofoil of Aspect Ratio = 4· Elastic Axis at 0·5*c*.

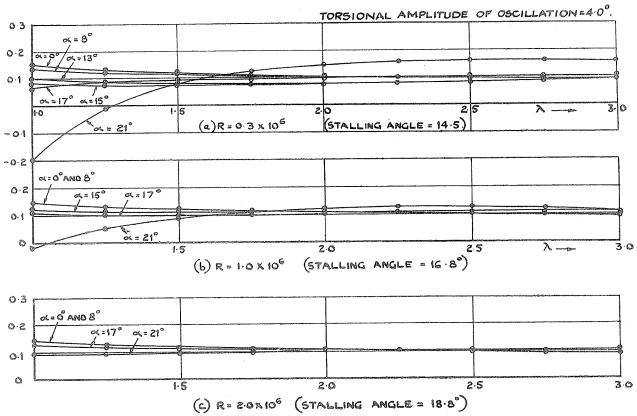

FIG. 29. Variation of j_3 with Incidence and Frequency Parameter at Various Reynolds numbers for an N.A.C.A. 0015 Aerofoil with Aspect Ratio = 6·0, and Elastic Axis at $0{\cdot}5c$.

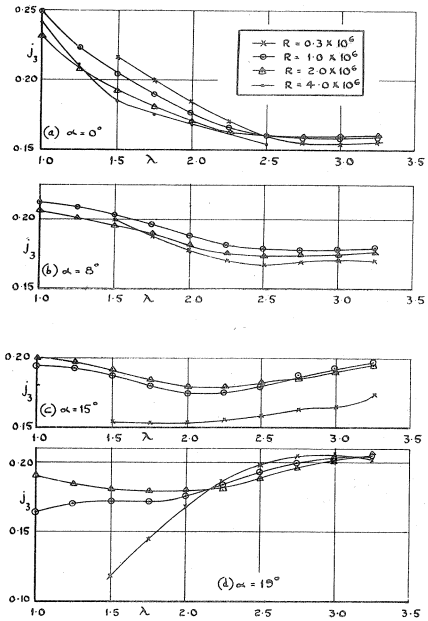

FIG. 30. Variation of j_3 with R and λ at Various Incidences.
N.A.C.A. 0015 Section $\theta_o = 4{\cdot}0°$.
Elastic Axis at $0{\cdot}33c$. Aspect Ratio $= 4{\cdot}8$

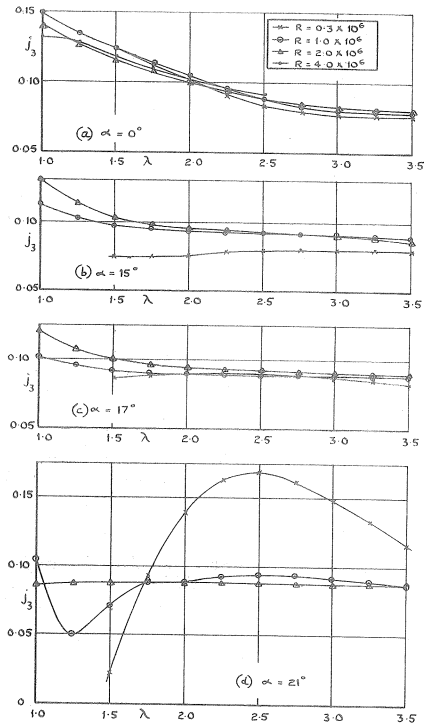

FIG. 31. Variation of j_3 with Reynolds number and Frequency Parameter λ at Various Incidences.
Section = N.A.C.A. 0015 $\theta_o = 4{\cdot}0°$
Elastic Axis at $0{\cdot}5c$. Aspect Ratio $= 4{\cdot}8$

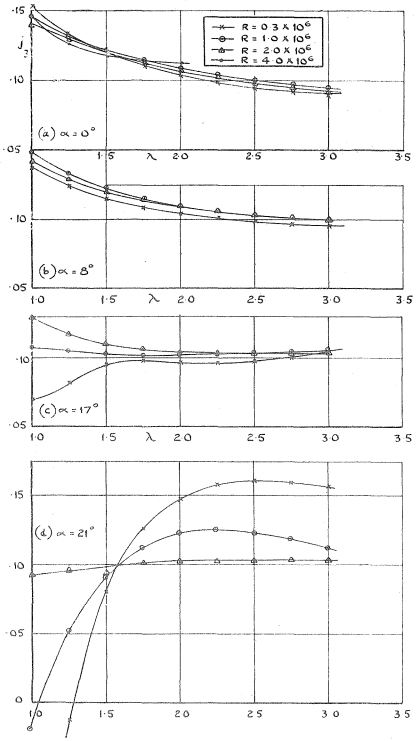

FIG. 32. Variation of j_3 with Reynolds number and Frequency Parameter, at Various Incidences.

Section = N.A.C.A. 0015 $\theta = 4{\cdot}0°$

Elastic Axis at $0{\cdot}5c$. Aspect Ratio = $6{\cdot}0$.

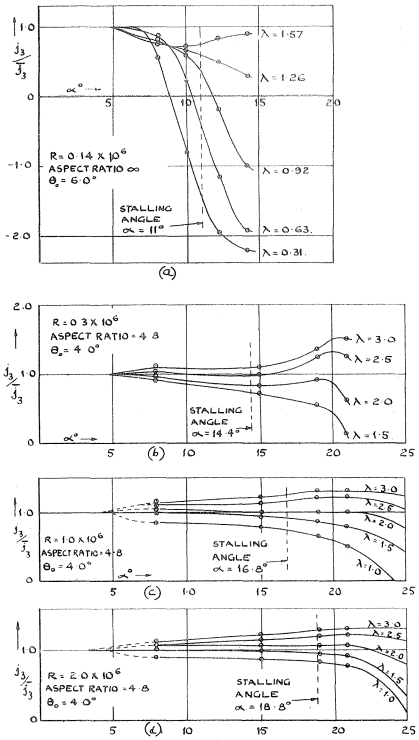

FIG. 33. Variation of the Ratio $j_3/\bar{j}_3$ with Incidence, for a Symmetric Aerofoil with Elastic Axis at $0{\cdot}33c$, and Various Values of the Reynolds number.

(Dotted lines show where shape of curve is uncertain.)

(74638) Wt. 9/7116 9/47 Hw. G377/1

Publications of the Aeronautical Research Committee

TECHNICAL REPORTS OF THE AERONAUTICAL RESEARCH COMMITTEE—

1934-35 Vol. I. Aerodynamics. 40*s.* (40*s.* 8*d.*)
Vol. II. Seaplanes, Structures, Engines, Materials, etc. 40*s.* (40*s.* 8*d.*)

1935-36 Vol. I. Aerodynamics. 30*s.* (30*s.* 7*d.*)
Vol. II. Structures, Flutter, Engines, Seaplanes, etc. 30*s.* (30*s.* 7*d.*)

1936 Vol. I. Aerodynamics General, Performance, Airscrews, Flutter and Spinning. 40*s.* (40*s.* 9*d.*)
Vol. II. Stability and Control, Structures, Seaplanes, Engines, etc. 50*s.* (50*s.* 10*d.*)

1937 Vol. I. Aerodynamics General, Performance, Airscrews, Flutter and Spinning. 40*s.* (40*s.* 9*d.*)
Vol. II. Stability and Control, Structures, Seaplanes, Engines, etc. 60*s.* (61*s.*)

ANNUAL REPORTS OF THE AERONAUTICAL RESEARCH COMMITTEE—

1933-34 1*s.* 6*d.* (1*s.* 8*d.*)
1934-35 1*s.* 6*d.* (1*s.* 8*d.*)
April 1, 1935 to December 31, 1936. 4*s.* (4*s.* 4*d.*)
1937 2*s.* (2*s.* 2*d.*)
1938 1*s.* 6*d.* (1*s.* 8*d.*)

INDEXES TO THE TECHNICAL REPORTS OF THE ADVISORY COMMITTEE ON AERONAUTICS—

December 1, 1936 — June 30, 1939
Reports & Memoranda No. 1850. 1*s.* 3*d.* (1*s.* 5*d.*)

July 1, 1939 — June 30, 1945
Reports & Memoranda No. 1950. 1*s.* (1*s.* 2*d.*)

Prices in brackets include postage.

Obtainable from

His Majesty's Stationery Office

London W.C.2: York House, Kingsway
[Post Orders—P.O. Box No. 569, London, S.E.1.]
Edinburgh 2: 13A Castle Street
Manchester 2: 39-41 King Street
Cardiff: 1 St. Andrew's Crescent
Belfast: 80 Chichester Street
or through any bookseller.

S.O. Code No. 23-2048